THE PUBLISHING HOUSE
OF THE ROMANIAN ACADEMY

PROCEEDINGS OF THE ROMANIAN ACADEMY, Series A,
Volume 18, Number 1/2017, pp. 42–49

MICRO-TOMOGRAPHY AND X-RAY ANALYSIS OF GEOLOGICAL SAMPLES

Ion GRUIA

University of Bucharest, Faculty of Physics, P.O. Box MG-11, RO-077125, Bucharest-Magurele, Romania
Corresponding author: Ion GRUIA, E-mail: gruia_ion@yahoo.com; ion.gruia@fizica.unibuc.ro

Abstract. The paper deals with the X-ray fluorescence (XRF) spectroscopy and the analysis of the elemental composition of geological samples (e.g. meteorite samples). The measurements were performed on several equipments to compare the results of sample elemental composition by using both X-ray and bremsstrahlung radiation. We designed a three-step analysis of the meteorite sample: (i) the initial XRF analysis, a non-destructive recognition in situ by micro-X-ray dispersive (μXRD) analysis to determine the mineralogical meteorite texture and to identify the features of interest followed by spatially correlated μXRD analysis, (ii) the XRF spectroscopy and the scanning electron microscopy-energy dispersive (SEM-EDX) analysis that is made in polished thin sections of the meteorite to know the mineralogical and the textural development, and finally (iii) the higher resolution mapping scanning electron microscopy on a smaller scale to correlate with the X-ray photoelectron spectroscopy (XPS) analysis of the meteorite sample.

Key words: XRF, X-ray microtomography (XRT), Scanning Electron Microprobe, SEM-EDX, XPS.

1. INTRODUCTION

When the electron beams interact with sample surfaces, it follows a series of signals that after being detected, amplified, and processed, allow us to obtain information on the morphology, structure, and composition of the samples. The signal obtained for imaging in a scanning electron microscopy (SEM) is not produced only from the surface of the sample analyzed. The electron beam penetrates a certain distance into the sample and can interact once or several times along its trajectory. The region of the sample between the original signal and the sub-sequential leakage that cannot be detected, is called the interaction volume [1, 2]. The resulting braking energy from these electrons is emitted in the form of X-ray photons that make up the continuous emission spectrum of the sample. The maximum intensity of continuous spectrum is determined by the acceleration voltage increase, the beam intensity, and the atomic number of the sample.

The meteorite sample analysis was done by several spectral methods to investigate the complex situations that may occur because there is the possibility of overlapping peaks with close energies, which can seriously hinder the whole analysis. Many such overlaps can be separated by de-convolution calculation peaks, but other more difficult problems may occur, e. g. some of the elements that can generate overlaps are found only in very small amounts in the sample composition. Using the electronic data system (EDS), all characteristic X-ray energies are measured simultaneously incident on the detector, and data acquisition is therefore very fast from one end to the other end of the whole spectrum. This is important for trace analysis of chemical elements [3, 4].

2. RESULTS AND DISCUSSION

2.1. The Micro-tomography and XRF analysis

We investigate three samples (ms, mfs, mc) of meteorite volume of $4\times4\times12$ mm^3. 3D investigation was made by acquiring 1 201 projections. The X-ray source-sample distance was 20 mm and the source-detector distance was 580 mm. The X-ray source has a W target operating system micro focus transmission, at 100 KV voltage and a current of 150 μA. Flat panel detector is of type Dexella with width of 1 944 pixels, with

height of 1 536 pixels, the pixel size of 74.8 μm, and 1 200 ms integration time. The devices used in this study are mainly represented in Figs. 1 and 2.

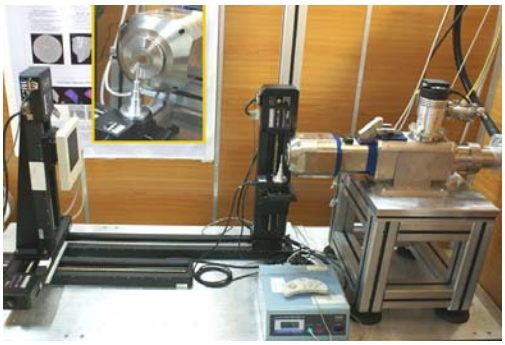

Fig. 1 – Experimental setup of micro-tomography method (http://tomography.inflpr.ro) [5].

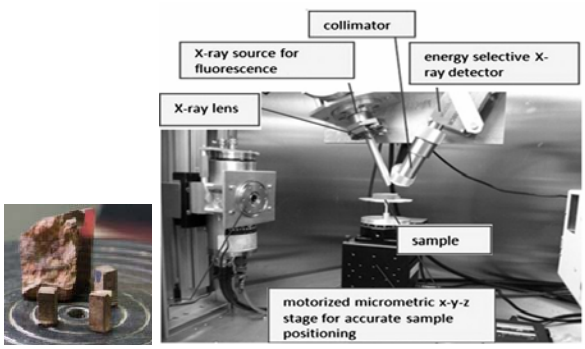

Fig. 2 – Photo of the non destructive method, to evaluate a X-ray fluorescence (XRF) technique (http://tomography.inflpr.ro) [5].

Positioning and turning around of the sample are ensured by a set of seven high-precision motorized micrometric manipulators. Automation, control, and data acquisition were obtained by means of an in-house software package. The tomography reconstruction for the cone-beam scanning is based on an optimized implementation of the modified cone-beam filtered back-projection algorithm (see Fig. 3).

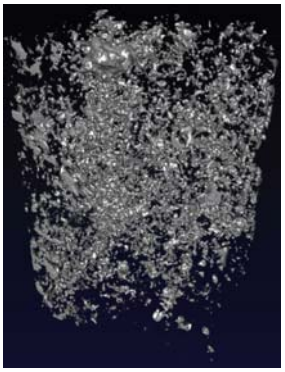

Fig. 3 – The tomography reconstruction.

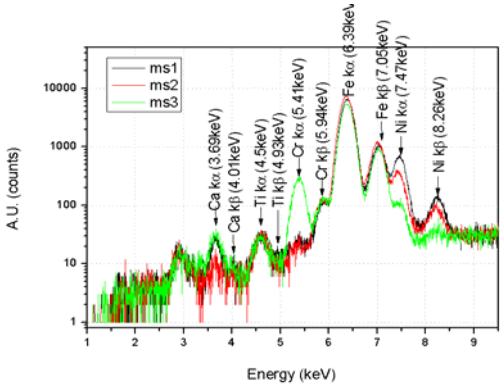

Fig. 4 – Measured energy spectrum from surface sample ”ms”.

The combination of analytical techniques used in the present study was useful for the following reasons: they are well suited in terms of the identification and location of inorganic elements in the meteorite sample. The corresponding graphs for the three investigated samples are obtained in the central area on the surface (1) and at a distance of 1 mm to the left (2), respectively, to the right (3) (see Figs. 4–6).

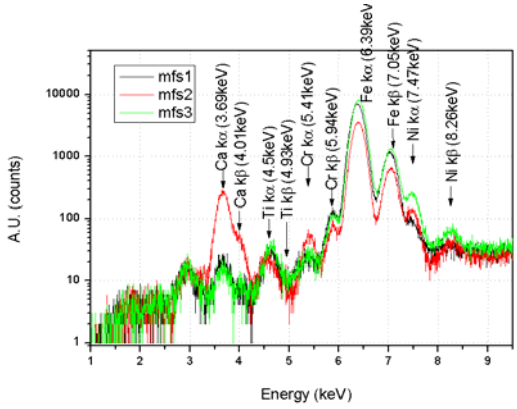

Fig. 5 – Measured energy spectrum from surface sample ”mfs”.

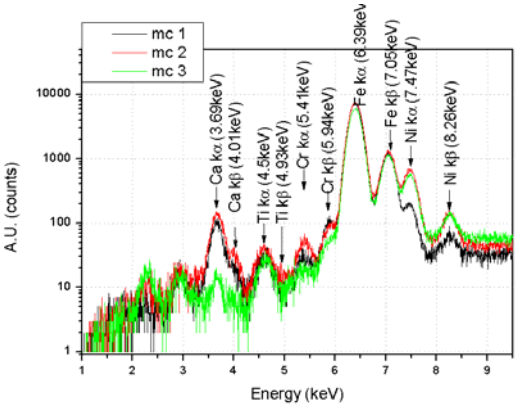

Fig. 6 – Measured energy spectrum from surface sample ”mc”.

It was determined that the X-ray micro tomography (XRT) is a powerful technique to observe on extended volumes the morphology, the alignment, and the local bulk density in samples.

2.2. The EDX analysis

The EDX spectrometers can be programmed to analyse the X-ray energy-dispersive spectrum while scanning the sample with the electron beam and with the possibility of obtaining results of compositional quality and quantity for a single point on the surface from a selected direction (the linear profile). Distributions across the entire surface of the analyzed chemical elements are also obtained. The very high efficiency and the uniform energy-dispersive analyses constitute the great advantage of these systems.

The material used in the present study was a bulk meteorite sliced into 10 plaques 1 mm thick and polished on both facets. So we got to study 20 polished surfaces, which are equidistant with a 1 mm step in order to get the component elements in the meteorite sample volume.

Experimental data for the EDX spectra were obtained in laboratories of various institutes (The National Institute for Laser, Plasma & Radiation Physics: INFLPR, National Institute for Materials Physics: NIMP, University Polytechnic of Bucharest: UPB, National Institute for Research and Development in Micro-technologies: IMT-Bucharest).

In general, the results obtained in scanning electron microscopy are only qualitative ones. However, we can take measurements of length, height, and depth of the micro details of relief and we can provide some angular relationships between topographic elements using stereoscopic image pairs. Such stereo-pairs are two micrographs of the same area taken before and after a slight change of angle of the sample (4−6°). Overlapping images into a stereo binocular allow us both obtaining the three-dimensional representation of the structure and the evaluation of geometrical parameters.

The experimental setup and the X-ray spectra used for the EDX analysis are shown in Figs. 7−15.

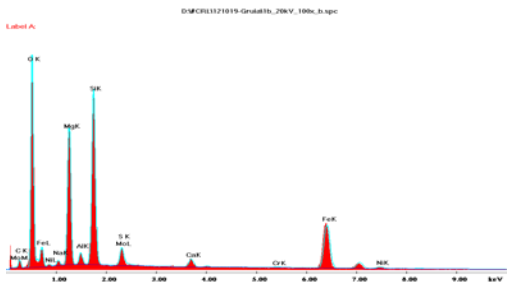

Fig. 7 – X-ray emission spectrum in the center of sample.

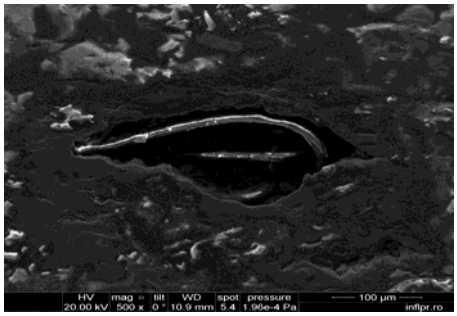

Fig. 8 – Investigated the meteorite sample surface (INFLPR).

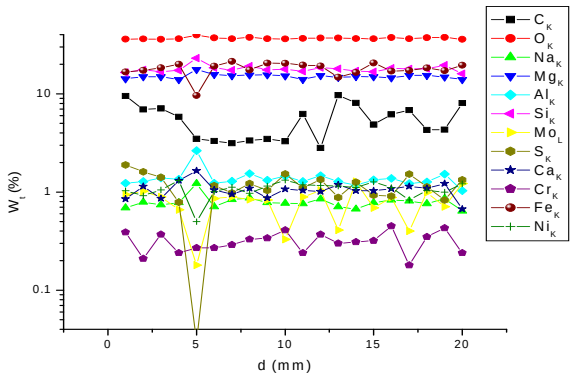

Fig. 9 – The distribution of elements on the surface of plane samples depending on the distance d in volume meteorite.

Fig. 10 – The certificate of origin of the meteorite.

The experimental EDX data for 20 polished surfaces, which are equidistant with a 1 mm step are summarized in Table 1 and are shown graphically in Fig. 9.

Table 1

Experimental EDX data for the estimation
of elements' content in the meteorite

Elem	Wt %												Total
d(mm)	C_K	O_K	Na_K	Mg_K	Al_K	Si_K	Mo_L	S_K	Ca_K	Cr_K	Fe_K	Ni_K	
1	9.51	36.07	0.69	14.26	1.23	16.48	0.94	1.89	0.85	0.39	16.66	1.03	100
2	6.93	36.26	0.79	14.94	1.28	17.55	1.02	1.61	1.14	0.21	17.34	0.92	100
3	7.10	36.03	0.74	14.92	1.39	16.83	0.89	1.41	0.86	0.37	18.41	1.05	100
4	5.83	36.37	0.78	14.00	1.35	17.34	0.66	0.79	1.31	0.24	20.03	1.31	100
5	3.48	39.69	1.22	17.67	2.64	23.07	0.18	0.03	1.65	0.27	9.60	0.50	100
6	3.31	37.06	0.71	15.73	1.23	18.44	0.86	1.16	1.05	0.27	19.17	1.01	100
7	3.14	36.39	0.84	15.31	1.29	17.40	0.89	0.98	0.95	0.29	21.38	1.12	100
8	3.34	37.62	0.87	15.56	1.54	19.14	0.84	1.22	1.09	0.33	17.48	0.97	100
9	3.46	36.46	0.78	15.61	1.32	17.59	0.83	1.04	0.87	0.34	20.55	1.15	100
10	3.30	36.28	0.77	15.25	1.45	17.84	0.33	1.53	1.07	0.41	20.47	1.32	100
11	6.23	36.64	0.76	14.05	1.28	16.97	0.89	1.10	1.04	0.24	19.61	1.19	100
12	2.81	36.94	0.85	15.34	1.47	18.46	1.04	1.34	1.01	0.37	19.20	1.17	100
13	9.68	36.95	0.71	14.69	1.28	17.97	0.41	0.88	1.19	0.30	14.79	1.15	100
14	8.10	36.53	0.67	14.99	1.17	17.07	1.28	1.26	1.03	0.31	16.48	1.11	100
15	4.86	36.39	0.78	14.97	1.33	16.78	0.69	0.93	1.03	0.32	20.66	1.27	100
16	6.18	37.41	0.83	14.52	1.38	18.22	0.88	0.91	1.08	0.45	17.02	1.11	100
17	6.82	36.46	0.81	15.41	1.22	17.94	0.40	1.52	1.14	0.18	17.27	0.83	100
18	4.28	37.24	0.76	15.40	1.27	18.07	0.99	1.13	1.09	0.35	18.37	1.04	100
19	4.33	37.53	0.86	14.80	1.52	19.55	0.71	0.83	1.22	0.43	17.22	1.00	100
20	8.06	36.03	0.64	13.95	1.03	16.05	1.22	1.33	0.67	0.24	19.57	1.21	100

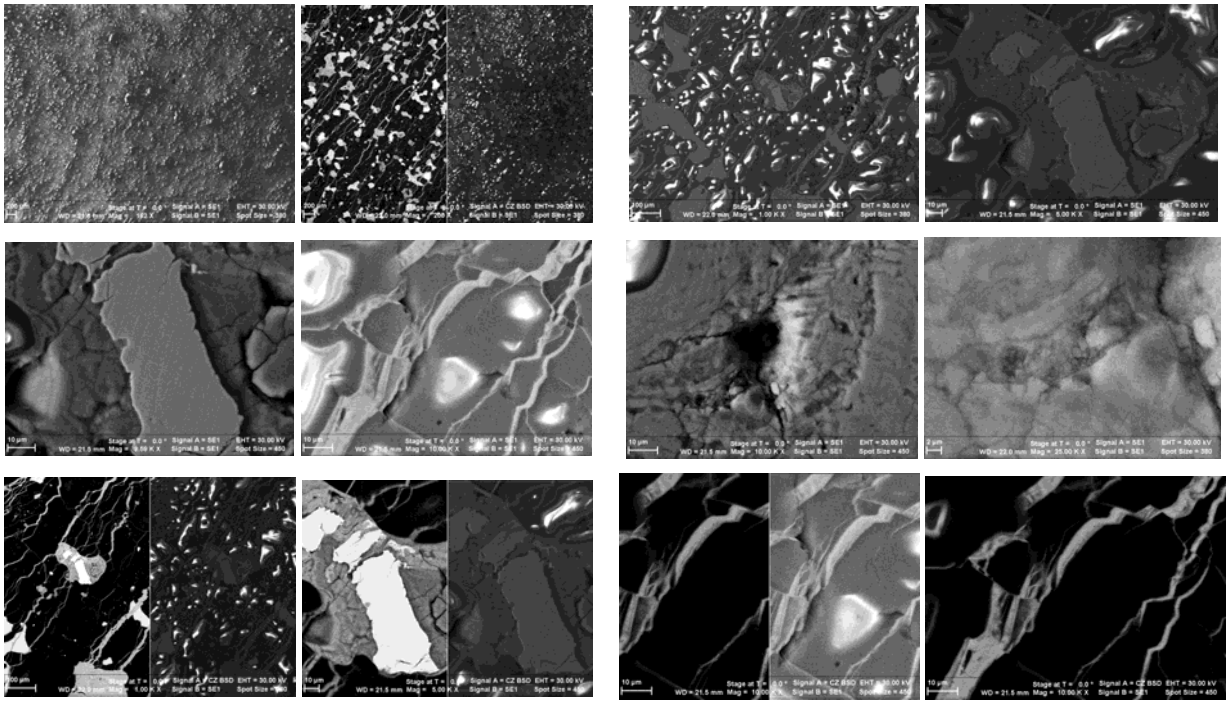

Fig. 11 – EDX images of meteorite for different magnitude (NIMP).

The experimental EDX data for different magnitudes are summarized in Table 2.

Table 2

Experimental data for the EDXRF estimation of elements in meteorite for different magnitudes (Fig. 11)

Elem	Wt %													Total
	Ni_K	Fe_K	Si_K	S_K	Ca_K	Mg_K	Al_L	Na_K	Cr_K	O_K	P_K	N_k	C_K	
200×	2.10	33.14	18.23	2.63	1.24	15.35	1.62	1.17	0.99	23.53				100
1000×	1.97	31.61	19.84	4.16	1.03	16.88	1.24	1.04	0.61	21.33	0.30			100
5000×	5.86	29.34	20.12	0.24	0.49	17.03	1.55	1.25	0.56	23.56	0.01			100
10000×	20.11	49.17	2.63			2.59	0.18			20.84			4.47	100
10000×	1.73	22.58	18.84		0.26	18.46	0.56			30.61		5.36	1.59	100

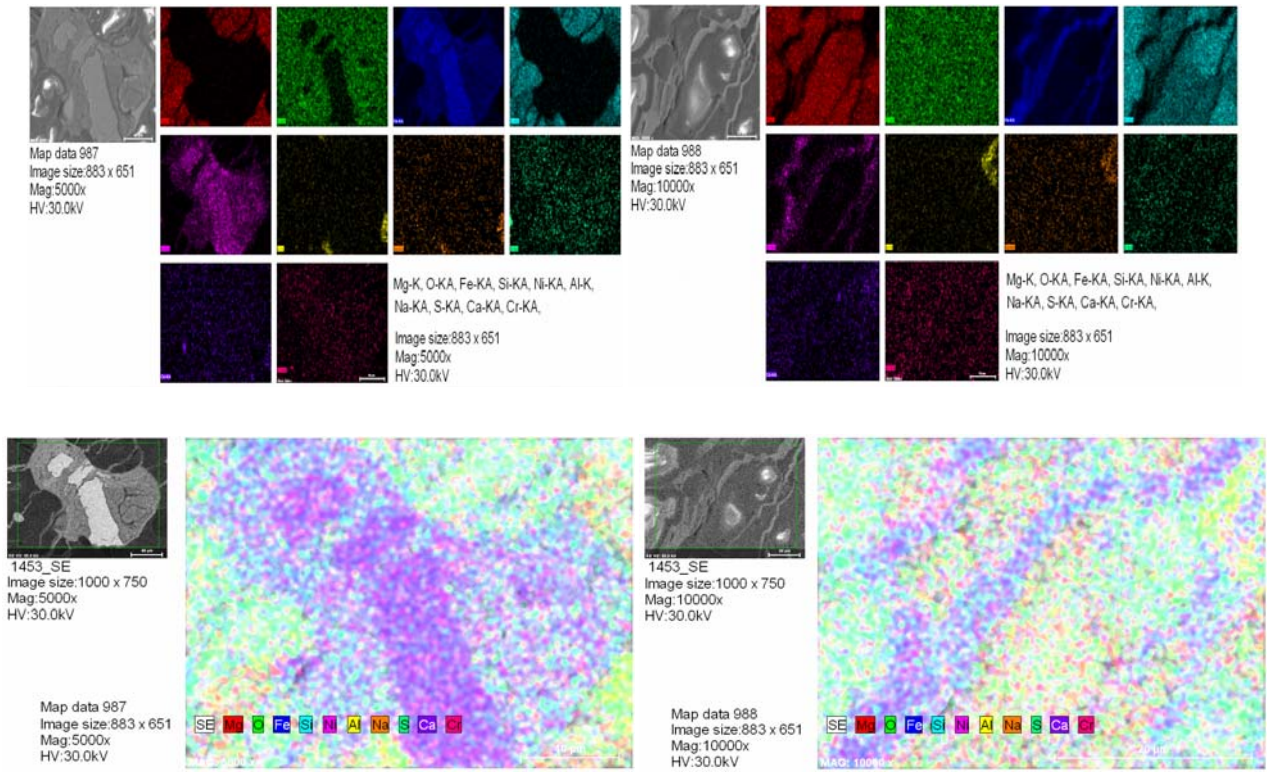

Fig. 12 – EDX element mapping in the meteorite (NIMP).

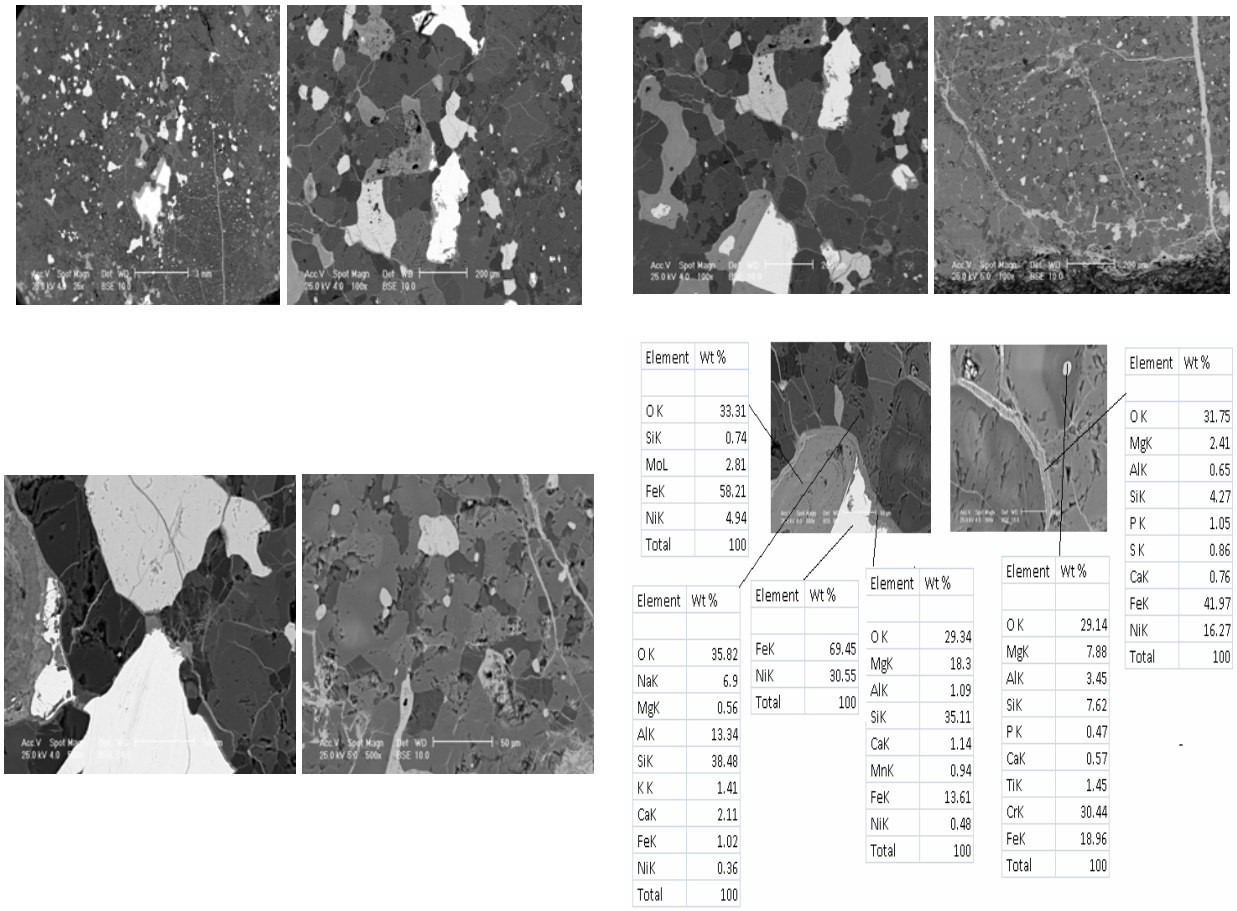

Element	Wt %
O K	33.31
Si K	0.74
Mo L	2.81
Fe K	58.21
Ni K	4.94
Total	100

Element	Wt %
O K	35.82
Na K	6.9
Mg K	0.56
Al K	13.34
Si K	38.48
K K	1.41
Ca K	2.11
Fe K	1.02
Ni K	0.36
Total	100

Element	Wt %
Fe K	69.45
Ni K	30.55
Total	100

Element	Wt %
O K	29.34
Mg K	18.3
Al K	1.09
Si K	35.11
Ca K	1.14
Mn K	0.94
Fe K	13.61
Ni K	0.48
Total	100

Element	Wt %
O K	29.14
Mg K	7.88
Al K	3.45
Si K	7.62
P K	0.47
Ca K	0.57
Ti K	1.45
Cr K	30.44
Fe K	18.96
Total	100

Element	Wt %
O K	31.75
Mg K	2.41
Al K	0.65
Si K	4.27
P K	1.05
S K	0.86
Ca K	0.76
Fe K	41.97
Ni K	16.27
Total	100

Fig. 13 – EDX images of meteorite for different magnitudes (UPB).

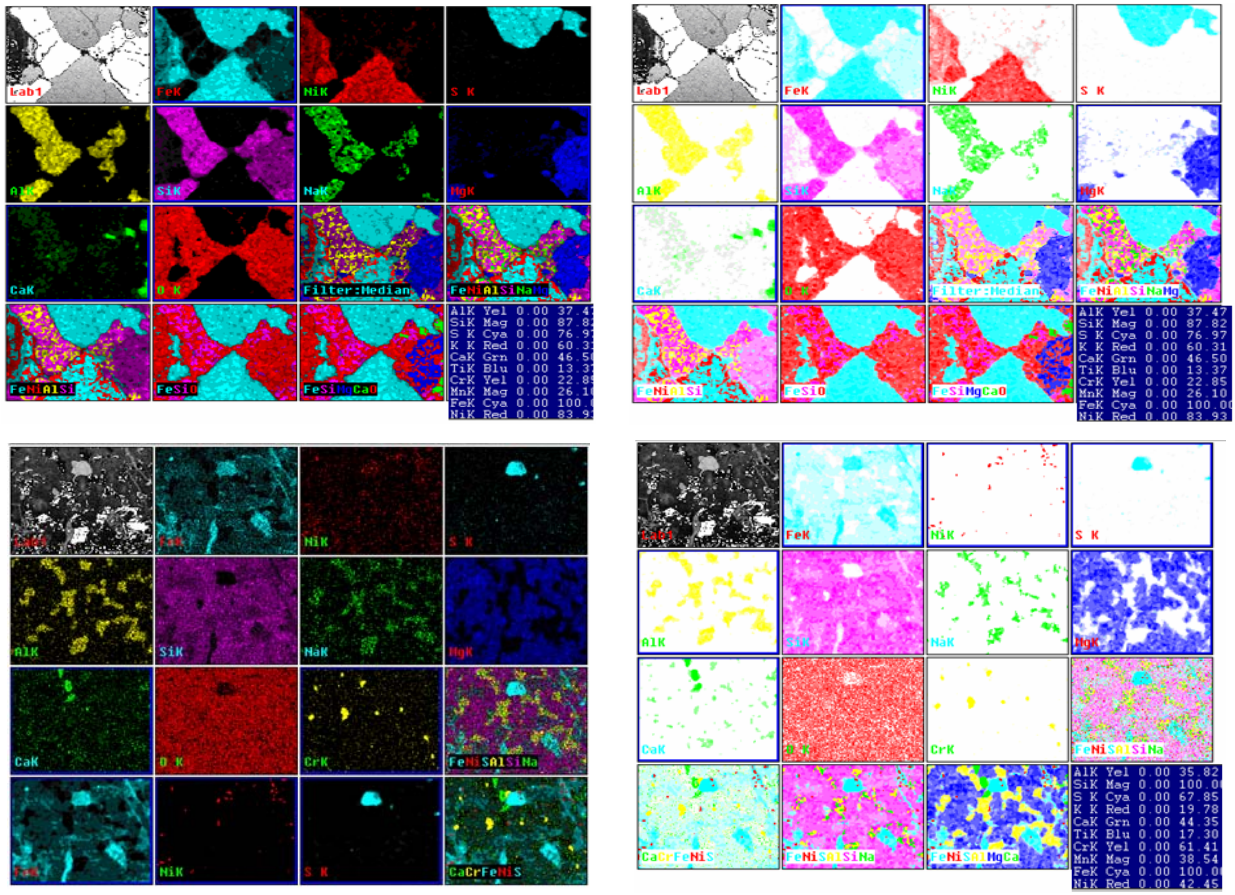

Fig. 14 – EDX element mapping in the meteorite (UPB).

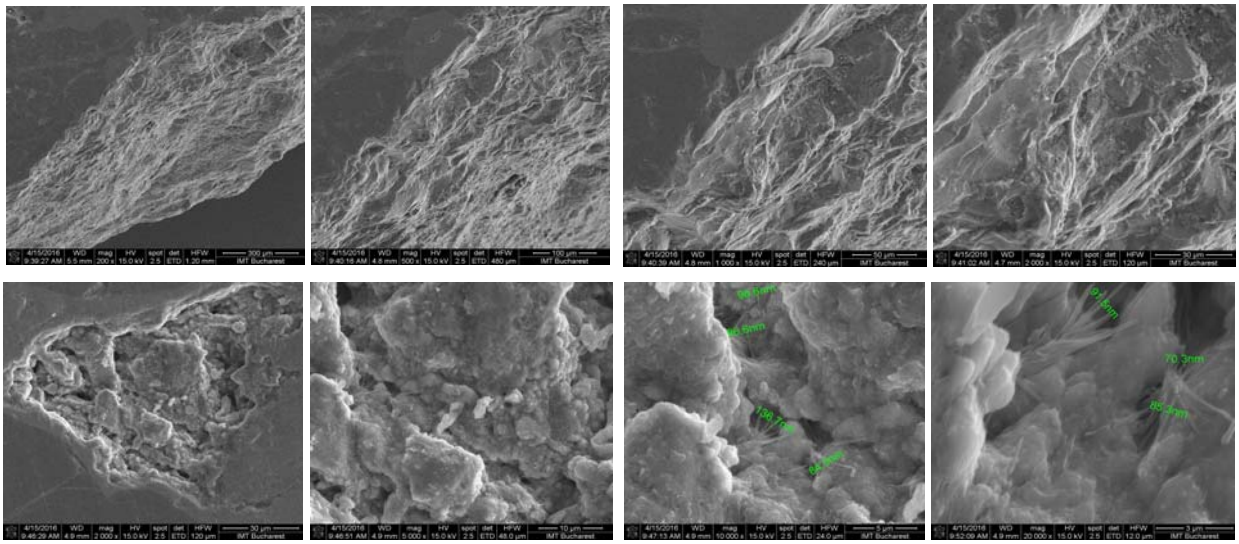

Fig. 15 – EDX images of meteorite for different magnitude (IMT).

2.3. The XPS analysis

X-ray photoelectron spectroscopy (XPS) is a spectroscopic technique based on photoelectric effect that measures the elemental composition, valence state, and electronic state of the elements that exist within a material. For XPS measurements, as accurate as possible, it is necessary to apply strict working procedures regarding sample preparation, instrument calibration, and processing of the obtained spectra. These procedures are described

in international standards and are required if we wish to obtain an accurate analysis. The XPS instrument measures the kinetic energy of all collected electrons. The electron signal includes contributions from both photoelectron and Auger electron lines. Surface analysis by XPS requires irradiating a solid in an ultra-high vacuum (UHV) chamber with mono-energetic soft X-rays and analyzing the energies of the emitted electrons [6].

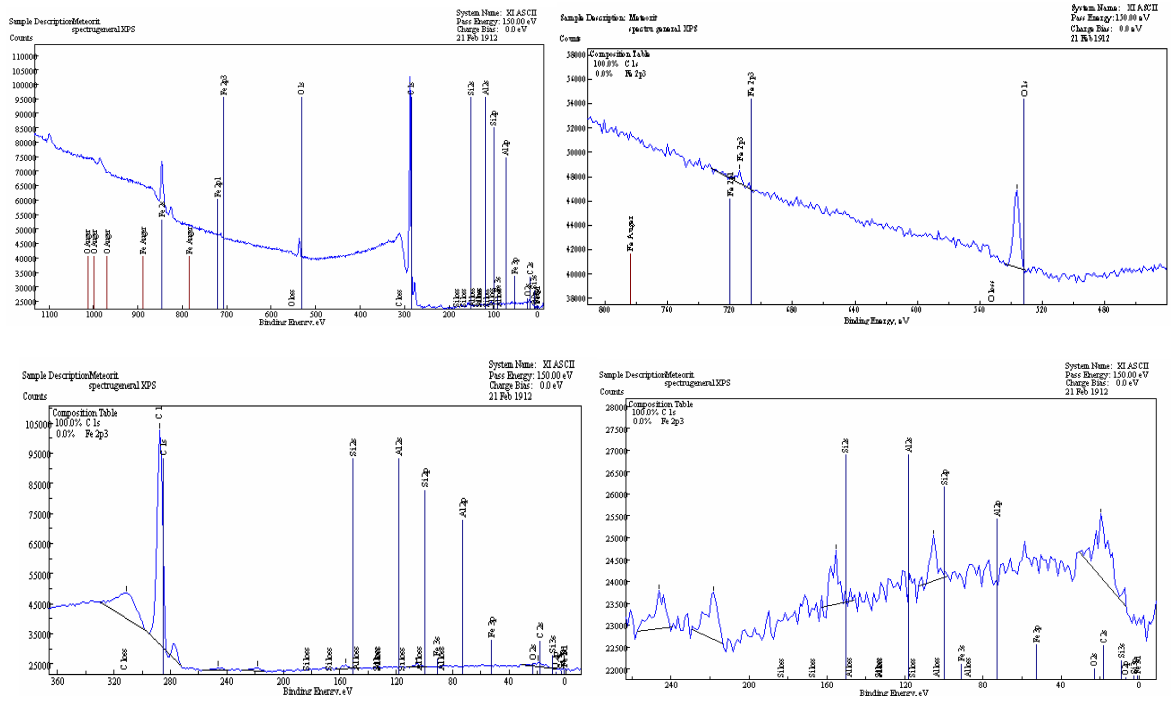

Fig. 16 – XPS spectrum of meteorite for different energy ranges (NIMP).

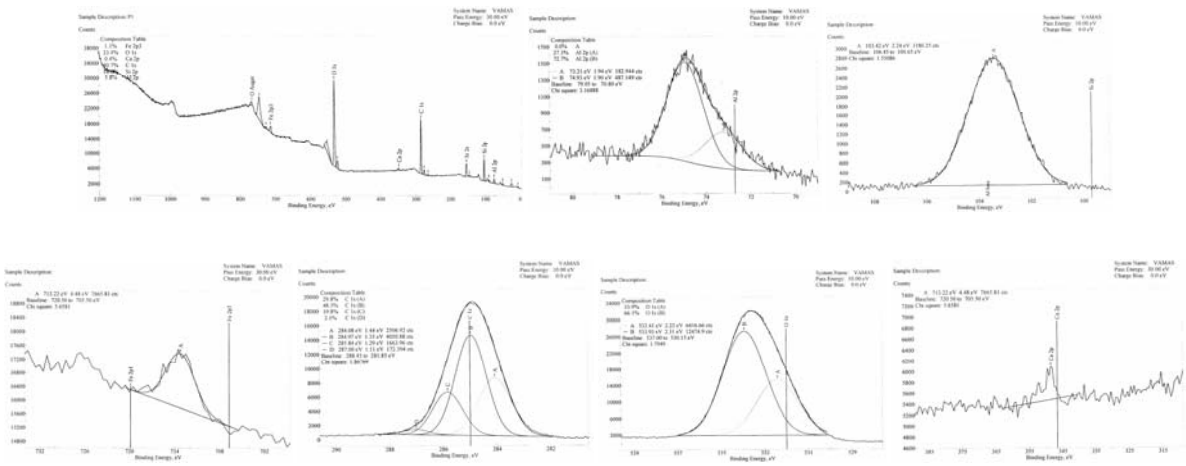

Fig. 17 – XPS spectrum of meteorite for different chemical elements (NIMP).

The experimental XPS data are summarized in Figs. 16 and 17.

3. CONCLUSIONS

In this paper we analyzed several pieces of a meteorite through photo and energy dispersion X-ray fluorescence (EDX) by using various analytical techniques and experimental methods. Combination of analytical techniques used in the present study was useful for the identification and location of inorganic elements in the meteorite sample. It is shown that X-ray micro tomography (XRT) is a powerful technique to observe on

extended volumes the morphology, alignment, and local bulk density in meteorite samples. Tomo-analytic combines a 3D X-ray micro-tomography with a micro beam fluorescence system. The micro beam fluorescence component is a configurable elemental composition mapping tool, including optical X-ray beam collimation. It is proved that the tomography analysis provides a substantial new information about pore connectivity. The photo-EDX and SEM analyses indicate that all components of the meteorite are clearly delimitated.

Further complementary results might be achieved on this meteorite sample by other related analytical techniques. Geological analysis of materials from diverse terrestrial environments and meteorites are investigated because they often retain excellent records relating to past processes such as earth genesis, climate change, and extreme events.

ACKNOWLEDGMENTS

The author wishes to thank many colleagues from the research laboratories institutes: INFLPR, NIMP, UPB, and IMT-Bucharest for the preparation of samples and for the related measurements.

REFERENCES

1. B.M. SIEGEL, D.R. BEAMAN, *Physical Aspects of Electron Microscopy and Microbeam Analysis*, New York, John Willey, 1975.
2. C.E. LYMAN *et al*., *Scanning Electron Microscopy, X-Ray Microanalysis and Analytical Electron Microscopy* (*A Laboratory Workbook*), Plenum Press, New-York, 1990.
3. S.J.B. REED, *Electron Probe Microanalysis*, 2nd ed., Cambridge University Press, 1993.
4. V.D. SCOTT, G. LOVE, S.J.B. REED, *Quantitative Electron-Probe Microanalysis*, 2nd ed., Ellis Horwood Limited, Hemel Hempstead, Hertfordshire, England, 1995.
5. http://tomography.inflpr.ro.
6. https://www.researchgate.net/publication/283316351_XRF_analysis_of_geological_materials.

Received June 6, 2016